

# Higgs Decay to Gluons at NNLO

Marco Schreck and Matthias Steinhauser

*Institut für Theoretische Teilchenphysik, Universität Karlsruhe (TH)  
76128 Karlsruhe, Germany*

## Abstract

We present an analytical calculation of the next-to-next-to-leading order corrections to the partial decay width  $H \rightarrow gg$  for a Higgs boson in the intermediate mass range. We apply an asymptotic expansion for  $M_H \ll 2M_t$  and compute three terms in the expansion. The leading term confirms the results present in the literature. It is argued that our result is equivalent to an exact calculation up to  $M_H \approx M_t$ . For a Higgs boson mass of 120 GeV the power-suppressed terms lead to corrections of about 9% in the next-to-next-to-leading order coefficient.

PACS numbers: 14.80.Bn 12.38.-t

# 1 Introduction

Up to date the Standard Model (SM) Higgs boson has evaded its direct detection. Electroweak precision data collected at the CERN Large Electron-Positron Collider (LEP), at the Stanford Linear Collider (SLC) and at the Tevatron at Fermilab predict a light SM Higgs boson below approximately 200 GeV. On the other hand, the direct search at LEP2 has excluded Higgs bosons below 114 GeV which leaves a relatively narrow window for the mass. A Higgs boson in this mass range, often also referred to as intermediate-mass Higgs boson, predominantly decays into bottom quarks and  $W$  bosons depending whether the latter decay is kinematically allowed. A further decay channel which is of phenomenological interest is the one into gluons. At lowest order this process is mediated by a top quark loop [1, 2]. The next-to-leading order (NLO) corrections are quite large and amount to roughly 70% [3–8]. About ten years ago the NNLO corrections have been computed in the limit of an infinitely heavy top quark mass [9, 10]. Since the corrections amount to approximately 20% they increased the reliability of the perturbative expansion of the decay rate. This has been further substantiated by the recent evaluation of the NNNLO corrections [11], again in the infinite top quark mass limit, which provides a contribution of about 2%.

The calculations to NNLO and NNNLO are both based on an effective theory which results from the SM after integrating out the top quark. The effective Lagrangian is constructed from operators with dimension five which is sufficient to obtain the leading term in the heavy-top expansion. The inclusion of higher-dimensional operators would lead to power-suppressed terms. However, the renormalization of the corresponding effective Lagrangian is quite tedious. In this paper we follow a different approach and consider the Higgs-boson propagator in the full SM. Its imaginary part leads — with the help of the optical theorem — directly to the decay rate. The disadvantage of this method is that at NNLO five-loop corrections to the Higgs two-point function have to be considered since the LO result already requires a three-loop diagram where the coupling of the Higgs boson to the gluons is mediated by two top quark triangles. They are connected by two gluon lines. The advantage of our method relies on the straightforward automatization using state-of-the-art techniques and program packages as we will show in Section 2.

An important feature of the Higgs boson decay into gluons is its affinity to the production mechanism in the gluon fusion channel. For the latter the NNLO corrections are again only known within the framework of the effective theory [12–14]. The calculation performed in the present paper gives a first hint about the potential size of the terms which are suppressed by the top quark mass.

Let us finally mention that the corresponding NNLO corrections to the decay of the Higgs boson into two photons have been obtained in Ref. [15]. Note that in this case a simple expansion of the Higgs-photon-photon vertex diagrams is sufficient to obtain power-suppressed terms the heavy  $M_t$ -limit. Thus only three- instead of five-loop diagrams have to be considered.

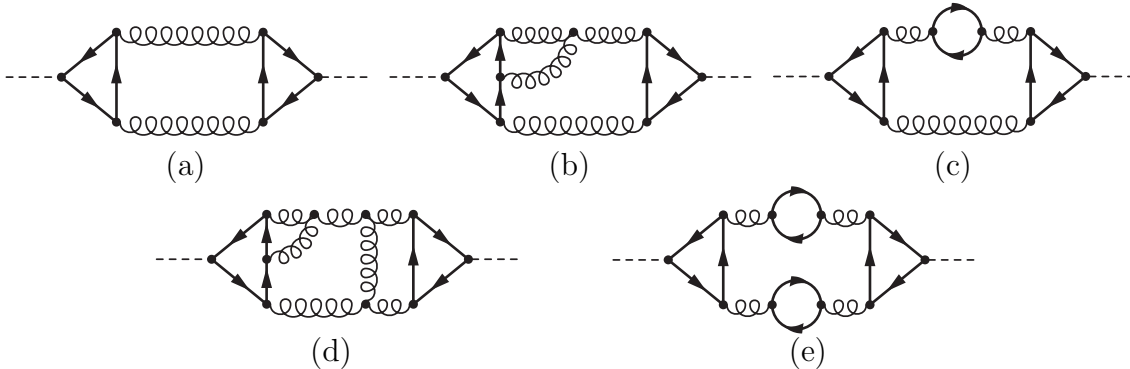


Figure 1: Sample diagrams contributing to  $\Pi_H$ . The curly lines represent gluons and the solid lines stand for light quarks or top quarks. The Higgs boson (external dashed lines) only couples to top quarks.

The paper is organized as follows: In Section 2 we present some details of our calculation and Section 3 contains our analytical results and the discussion about the numerical implications. We conclude the paper with Section 4.

## 2 The calculation

As already mentioned in the Introduction, for the computation of the decay rate  $\Gamma(H \rightarrow gg)$  we consider the Higgs boson self energy,  $\Pi_H(q^2)$ , and apply the optical theorem which in our case reads

$$\Gamma(H \rightarrow gg) = \frac{1}{M_H} \text{Im} [\Pi_H(M_H^2 + i0)] . \quad (1)$$

Since we do not consider the (exclusive) decay into light quarks only those diagrams contribute to  $\Pi_H$  where the Higgs boson couples to the top quark. Thus the LO result is obtained from the three-loop diagram shown in Fig. 1(a) (and the one with crossed gluons). The NLO and NNLO results are obtained by dressing this diagram with additional gluons and (light and heavy) quark loops. Sample diagrams can be found in Fig. 1(b)–(e). It is clear that beyond LO next to gluons also light quarks can be produced. In particular, at NNLO also a final state  $q\bar{q}q'\bar{q}'$  with light quark flavours  $q$  and  $q'$  is possible.

Our approach for the computation of  $\Gamma(H \rightarrow gg)$  requires the evaluation of five-loop diagrams in order to obtain the NNLO corrections. With the currently available techniques their exact evaluation is out of reach. However, for a Higgs boson in the intermediate mass range it is promising to consider an expansion for  $M_H^2 \ll M_t^2$  which shows a rapid convergence at LO and NLO as we demonstrate in Section 3. In this limit we can apply the so-called hard-mass procedure (see, e.g., Ref. [16]) to the propagator diagrams which then factorize into products of one-, two- and three-loop integrals. A graphical example

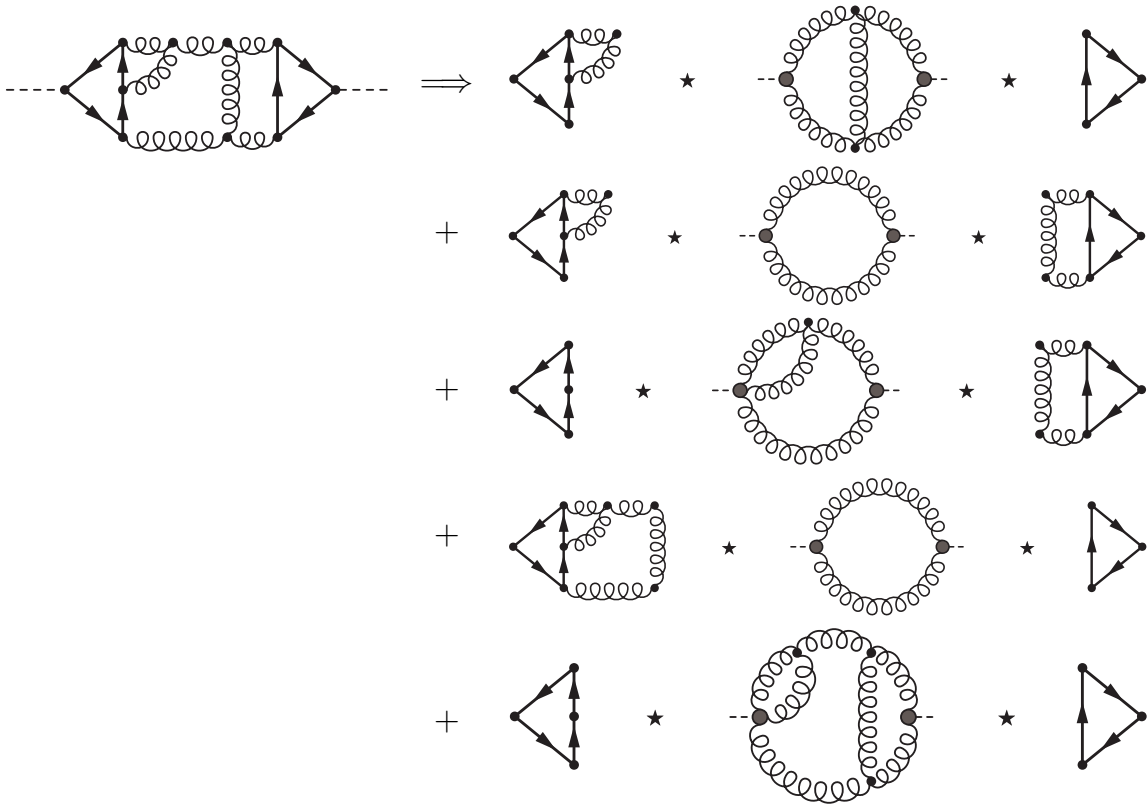


Figure 2: Sample five-loop diagram contribution to  $\Pi_H$  where the hard-mass procedure is applied in graphical form. Only the subgraphs contributing to the imaginary part are shown.

is shown in Fig. 2 where — according to the rules of the hard-mass procedure — five subdiagrams are identified. They have to be expanded in the small quantities and then to be inserted in the co-subgraph which (in this example) only consists of gluons. In Fig. 2 they are sandwiched between the symbols “ $\star$ ”. The hard-mass procedure has been automated in the program `exp` [17, 18] which we use for our calculation.

At LO we have two contributing Feynman diagrams, at NLO there are already 71 and at NNLO 2649. All Feynman diagrams are generated with `QGRAF` [19] and the various topologies are identified with the help of `q2e` [17, 18]. Afterwards `exp` [17, 18] applies the hard-mass expansion and produces output which can be read by the `FORM` [20] packages `MATAD` [21] and `MINCER` [22]. `MATAD` can compute vacuum integrals up to three-loop order where in our case the mass scale is given by the top quark. On the other hand, `MINCER` can handle massless propagator-type diagrams where for our application the external momentum is given by the Higgs boson mass.

According to the optical theorem we have to compute the imaginary part of  $\Pi_H$  which requires the evaluation of the pole part of the three-, four- and five-loop diagrams. Since **MATAD** and **MINCER** are constructed such that at most the finite parts of three-loop diagrams can be computed slight modifications are necessary which allow the correct evaluation of the  $1/\epsilon$  pole part of the five-loop diagrams.

For some of the diagrams it turned out to be crucial to use the parallel versions of **FORM** — **ParFORM** [23] and **TFORM** [24] — in order to obtain results in a moderate amount of time. With our setup, which is not tuned for a parallel computation, we obtain speedup factors between four and five using eight processors.

## 3 Results and discussion

### 3.1 LO and NLO result

The method described in the previous Section can be tested at LO and NLO where the exact results are known. Let us for this purpose introduce the notation

$$\Gamma(H \rightarrow gg) = \Gamma_0 \left( \frac{\alpha_s(\mu)}{\pi} \right)^2 \left[ \Gamma_{gg}^{\text{LO}} + \frac{\alpha_s(\mu)}{\pi} \Delta\Gamma_{gg}^{\text{NLO}} + \left( \frac{\alpha_s(\mu)}{\pi} \right)^2 \Delta\Gamma_{gg}^{\text{NNLO}} + \dots \right], \quad (2)$$

with  $\Gamma_0 = G_F M_H^3 / (36\pi\sqrt{2})$ .  $\Gamma_{gg}^{\text{LO}}$  is given by [1, 2]

$$\begin{aligned} \Gamma_{gg}^{\text{LO}} &= \left[ \frac{3}{2\tau} \left( 1 + \left( 1 - \frac{1}{\tau} \right) \arcsin^2 \sqrt{\tau} \right) \right]^2 \\ &= 1 + \frac{7}{15}\tau + \frac{1543}{6300}\tau^2 + \frac{226}{1575}\tau^3 + \frac{55354}{606375}\tau^4 + \frac{1461224}{23648625}\tau^5 + \dots, \end{aligned} \quad (3)$$

with  $\tau = M_H^2 / (4M_t^2)$  where  $M_t$  is the on-shell quark mass. In the second line of Eq. (3) we have performed an expansion up to order  $\tau^5$  which we could confirm by applying the hard-mass procedure to the three-loop diagrams (cf. Fig 1(a)). The ellipses indicate higher order terms in  $\tau$ .

The exact NLO result is only known in numerical form [4–8]. Thus we concentrate on the expansion for  $M_H \ll 2M_t$ . The first three terms have been computed in Ref. [25] which we could confirm. Furthermore, we have added two more terms and arrive at

$$\Delta\bar{\Gamma}_{gg}^{\text{NLO}} = h_0^{\text{nlo}} + h_1^{\text{nlo}}\bar{\tau} + h_2^{\text{nlo}}\bar{\tau}^2 + h_3^{\text{nlo}}\bar{\tau}^3 + h_4^{\text{nlo}}\bar{\tau}^4 + h_5^{\text{nlo}}\bar{\tau}^5 + \dots, \quad (4)$$

where

$$\begin{aligned}
h_0^{\text{nlo}} &= \frac{95}{4} + \frac{11}{2}L_H + n_l \left( -\frac{7}{6} - \frac{L_H}{3} \right), \\
h_1^{\text{nlo}} &= \frac{5803}{540} + \frac{77}{30}L_H - \frac{14}{15}L_t + n_l \left( -\frac{29}{60} - \frac{7}{45}L_H \right), \\
h_2^{\text{nlo}} &= \frac{1029839}{189000} + \frac{16973}{12600}L_H - \frac{1543}{1575}L_t + n_l \left( -\frac{89533}{378000} - \frac{1543}{18900}L_H \right), \\
h_3^{\text{nlo}} &= \frac{9075763}{2976750} + \frac{1243}{1575}L_H - \frac{452}{525}L_t + n_l \left( -\frac{3763}{28350} - \frac{226}{4725}L_H \right), \\
h_4^{\text{nlo}} &= \frac{50854463}{27783000} + \frac{27677}{55125}L_H - \frac{442832}{606375}L_t + n_l \left( -\frac{10426231}{127338750} - \frac{55354}{1819125}L_H \right), \\
h_5^{\text{nlo}} &= \frac{252432553361}{218513295000} + \frac{730612}{2149875}L_H - \frac{2922448}{4729725}L_t \\
&\quad + n_l \left( -\frac{403722799}{7449316875} - \frac{1461224}{70945875}L_H \right), \tag{5}
\end{aligned}$$

with  $L_H = \ln(\mu^2/M_H^2)$  and  $L_t = \ln(\mu^2/m_t^2)$ . In Eq. (4) we have  $\bar{\tau} = M_H^2/(4m_t^2)$  where  $m_t \equiv m_t(\mu)$  is the  $\overline{\text{MS}}$  top quark mass. For convenience we have kept the label referring to closed light-quark loops which takes the numerical value  $n_l = 5$ . Furthermore, we have  $\alpha_s(\mu) \equiv \alpha_s^{(5)}(\mu)$ , i.e., the top quark has been decoupled from the running of the strong coupling (see, e.g., Ref. [10]).

Transforming the top quark mass from the  $\overline{\text{MS}}$  to the on-shell scheme [26] leads to the following result which is evaluated in numerical form

$$\begin{aligned}
\Delta\Gamma_{gg}^{\text{NLO}} &= 17.9167 + 3.83333L_H + (9.574 + 1.789L_H)\tau \\
&\quad + (5.571 + 0.939L_H)\tau^2 + (3.533 + 0.550L_H)\tau^3 \\
&\quad + (2.395 + 0.350L_H)\tau^4 + (1.708 + 0.237L_H)\tau^5 + \dots \tag{6}
\end{aligned}$$

In Fig. 3  $\Gamma_{gg}^{\text{LO}}$  is shown as a function of  $\tau$  (solid line) and compared to the approximations where successively higher orders are included (dashed lines). The analog plots for the NLO results  $\Delta\bar{\Gamma}_{gg}^{\text{NLO}}$  and  $\Delta\Gamma_{gg}^{\text{NLO}}$  are shown in Fig. 4 where  $\mu^2 = M_H^2$  has been chosen. From the behaviour of the approximations we can deduce that in the region, where the curves including different orders in the  $M_t$ -expansion are on top of each other, they also coincide with the exact result. Having this in mind we conclude for the NLO corrections that in case of the pole mass the approximations including the  $\tau^5$  ( $\tau^2$ ) terms coincide with the exact result up to  $\tau \approx 0.60$  (0.35) which corresponds to  $M_H \approx 270$  (200) GeV. It is worth to mention that the top quark mass-suppressed corrections become smaller if the  $\overline{\text{MS}}$  mass is used for the parameterization. In this case the curves including the  $\bar{\tau}^4$  and  $\bar{\tau}^5$  terms, respectively, are basically on top of each other — almost up to  $\bar{\tau} = 1$ . Even the curve including corrections up to order  $\bar{\tau}^2$  shows a deviation of less than 6% for  $\bar{\tau} = 1$  and provides a perfect approximation up to  $\bar{\tau} = 0.5$  (i.e.  $M_H \approx 250$  GeV). Thus, it can

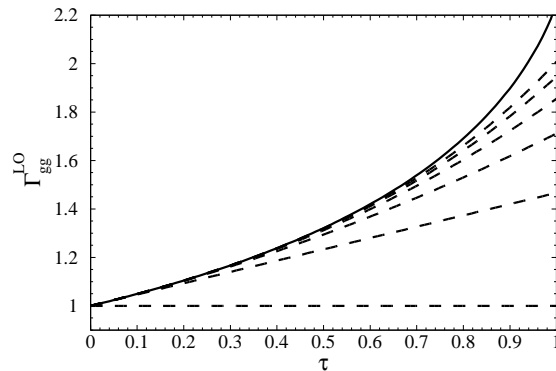


Figure 3:  $\Gamma_{gg}^{\text{LO}}$  as a function of  $\tau$  where successively higher orders are included (dashed lines). The exact result is shown as a solid line.

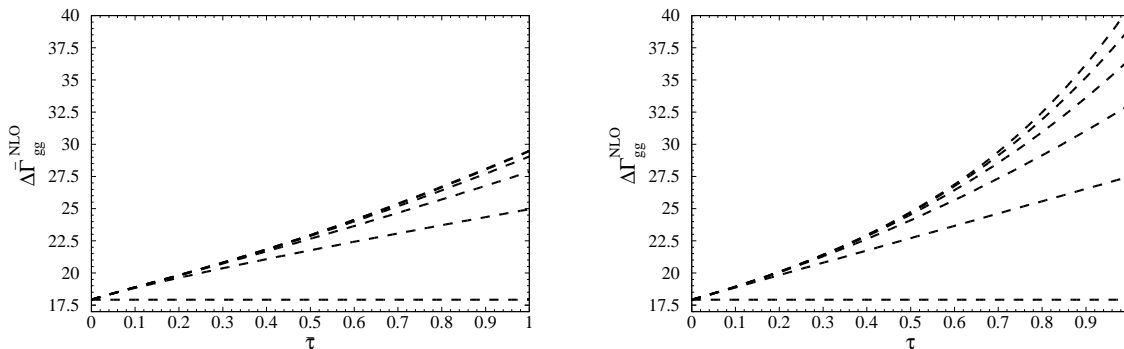


Figure 4:  $\Delta\bar{\Gamma}_{gg}^{\text{NLO}}$  (left) and  $\Delta\Gamma_{gg}^{\text{NLO}}$  (right) as a function of  $\bar{\tau}$  and  $\tau$ , respectively, where successively higher orders are included. For the renormalization scale  $\mu^2 = M_H^2$  has been chosen.

be assumed that in the phenomenologically relevant region for  $M_H$  the results including the first three expansion terms in  $\tau$  represent an excellent approximation for all practical purposes. Let us also mention that for  $M_H = 120$  GeV (corresponding to  $\tau \approx 0.1$ ) the leading term in the  $1/M_t$  expansion approximates the exact result with an accuracy of about 5% — both for the on-shell and  $\overline{\text{MS}}$  top quark mass. These considerations provide a strong motivation to compute the first three expansion terms at NNLO.

Very often, in particular in the context of the Higgs boson production in the gluon fusion process, the complete LO result is factored out when considering the perturbative

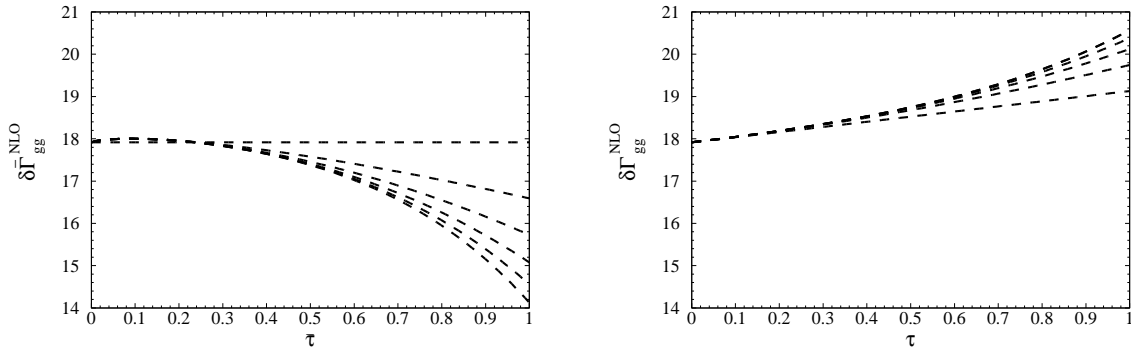


Figure 5:  $\delta\bar{\Gamma}_{gg}^{\text{NLO}}$  (left) and  $\delta\Gamma_{gg}^{\text{NLO}}$  (right) as a function of  $\bar{\tau}$  and  $\tau$ , respectively, where successively higher orders are included. For the renormalization scale  $\mu^2 = M_H^2$  has been chosen.

expansion. In this case we define

$$\Gamma(H \rightarrow gg) = \Gamma_0 \left( \frac{\alpha_s(\mu)}{\pi} \right)^2 \Gamma_{gg}^{\text{LO}} \left[ 1 + \frac{\alpha_s(\mu)}{\pi} \delta\Gamma_{gg}^{\text{NLO}} + \left( \frac{\alpha_s(\mu)}{\pi} \right)^2 \delta\Gamma_{gg}^{\text{NNLO}} + \dots \right]. \quad (7)$$

The coefficients  $\delta\Gamma_{gg}^{\text{NLO}}$  — both in the  $\overline{\text{MS}}$  and on-shell scheme — can easily be obtained from the results for  $\Delta\Gamma_{gg}^{\text{NLO}}$ . We refrain from listing them explicitly.

In Fig. 5  $\delta\bar{\Gamma}_{gg}^{\text{NLO}}$  and  $\delta\Gamma_{gg}^{\text{NLO}}$  are shown as a function of  $\bar{\tau}$  and  $\tau$ , respectively, where successively higher orders are included. One observes a dramatic improvement in the convergence of the  $1/M_t$  expansion for  $\tau \lesssim 0.3$  where already the leading  $M_t$ -term is practically indistinguishable from the exact result.

### 3.2 $H \rightarrow gg$ to NNLO

Applying the methods described in Section 2 to the five-loop diagrams shown in Fig. 1 leads to the NNLO corrections to the decay rate  $\Gamma(H \rightarrow gg)$ . We were able to compute three expansion terms in  $\tau$  which can be cast in the form

$$\Delta\bar{\Gamma}_{gg}^{\text{NNLO}} = h_0^{\text{nnlo}} + h_1^{\text{nnlo}}\bar{\tau} + h_2^{\text{nnlo}}\bar{\tau}^2 + \dots, \quad (8)$$

with

$$\begin{aligned}
h_0^{\text{nnlo}} &= \frac{149533}{288} - \frac{121}{16}\pi^2 - \frac{495}{8}\zeta(3) + \frac{3301}{16}L_H + \frac{363}{16}L_H^2 + \frac{19}{8}L_t + n_l \left( -\frac{4157}{72} + \frac{11}{12}\pi^2 \right. \\
&\quad \left. + \frac{5}{4}\zeta(3) - \frac{95}{4}L_H - \frac{11}{4}L_H^2 + \frac{2}{3}L_t \right) + n_l^2 \left( \frac{127}{108} - \frac{\pi^2}{36} + \frac{7}{12}L_H + \frac{L_H^2}{12} \right), \\
h_1^{\text{nnlo}} &= \frac{104358341}{1555200} - \frac{847}{240}\pi^2 + \frac{7560817}{69120}\zeta(3) + L_H \left( \frac{203257}{2160} - \frac{77}{15}L_t \right) + \frac{847}{80}L_H^2 \\
&\quad - \frac{24751}{1080}L_t - \frac{77}{180}L_t^2 + n_l \left[ -\frac{9124273}{388800} + \frac{77}{180}\pi^2 + \frac{7}{12}\zeta(3) + L_H \left( -\frac{67717}{6480} \right. \right. \\
&\quad \left. \left. + \frac{14}{45}L_t \right) - \frac{77}{60}L_H^2 + \frac{586}{405}L_t + \frac{7}{90}L_t^2 \right] + n_l^2 \left( \frac{5597}{12960} - \frac{7}{540}\pi^2 + \frac{29}{120}L_H \right. \\
&\quad \left. + \frac{7}{180}L_H^2 \right), \\
h_2^{\text{nnlo}} &= -\frac{1279790053883}{12192768000} - \frac{186703}{100800}\pi^2 + \frac{39540255113}{232243200}\zeta(3) + L_H \left( \frac{9158957}{189000} \right. \\
&\quad \left. - \frac{16973}{3150}L_t \right) + \frac{186703}{33600}L_H^2 - \frac{10980293}{453600}L_t + \frac{20059}{37800}L_t^2 + n_l \left[ -\frac{64661429393}{5715360000} \right. \\
&\quad \left. - \frac{16973}{25200}L_H^2 + \frac{16973}{75600}\pi^2 + \frac{1543}{5040}\zeta(3) + L_H \left( -\frac{10306537}{1944000} + \frac{1543}{4725}L_t \right) \right. \\
&\quad \left. + \frac{8973773}{6804000}L_t + \frac{1543}{18900}L_t^2 \right] + n_l^2 \left( \frac{3829289}{19440000} - \frac{1543}{226800}\pi^2 + \frac{89533}{756000}L_H \right. \\
&\quad \left. + \frac{1543}{75600}L_H^2 \right), \tag{9}
\end{aligned}$$

where the  $\overline{\text{MS}}$  top quark mass has been used. Transforming the result to the on-shell scheme and evaluating it in numerical form leads to

$$\begin{aligned}
\Delta\Gamma_{gg}^{\text{NNLO}} &= 156.808 + 102.146L_H + 11.021L_H^2 + 5.708L_T + \\
&\quad (109.365 + 52.662L_H + 5.143L_H^2 + 4.645L_T)\tau + \\
&\quad (74.434 + 29.920L_H + 2.699L_H^2 + 3.297L_T)\tau^2 + \dots, \tag{10}
\end{aligned}$$

with  $L_T = \ln(\mu^2/M_t^2)$ . We want to mention that the result for  $h_0^{\text{nnlo}}$  has already been obtained in Ref. [9, 10], the remaining terms are new.

Let us for completeness mention that the leading term of the large top quark mass expansion is also known at NNNLO [11]. It is given by

$$\begin{aligned}
\Delta\Gamma_{gg}^{\text{NNNLO}} &= 467.684 + 1215.302L_H + 394.514L_H^2 + 28.164L_H^3 \\
&\quad + 21.882L_HL_T + 122.441L_T + 10.941L_T^2 + \dots \tag{11}
\end{aligned}$$

In Fig. 6 we show the results of Eqs. (8) and (10). For small values of  $\tau$  one observes a logarithmic divergence which even occurs for  $\mu = M_H$ . In the phenomenologically relevant

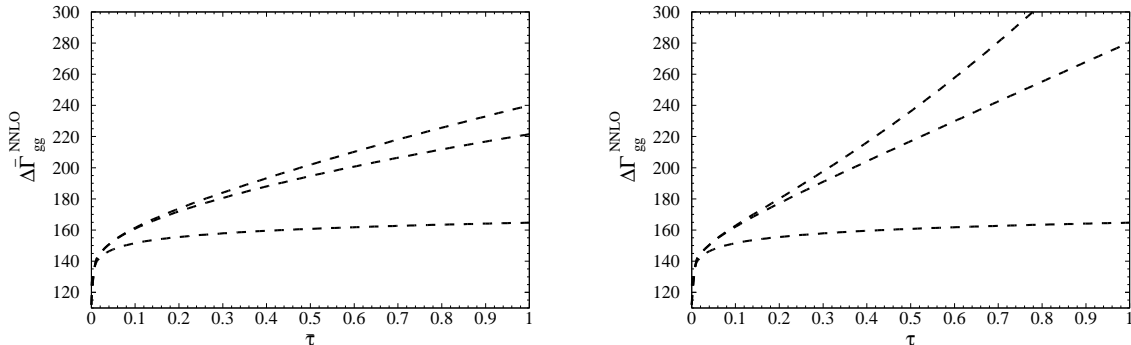


Figure 6:  $\Delta\bar{\Gamma}_{gg}^{\text{NNLO}}$  (left) and  $\Delta\Gamma_{gg}^{\text{NNLO}}$  (right) as a function of  $\bar{\tau}$  and  $\tau$ , respectively, where successively higher orders are included. For the renormalization scale  $\mu^2 = M_H^2$  has been chosen.

range ( $\tau \gtrsim 0.1$ ) the logarithm  $\ln(M_H^2/M_t^2)$  is numerically small and we observe the same pattern as at LO and NLO which is a strong indication that our result including the  $\tau^2$  terms provides an excellent approximation to the exact result up to  $M_H \approx M_t$  ( $\tau \approx 0.25$ ). For  $M_H = 120$  GeV ( $\tau \approx 0.1$ ) we observe a correction of about 9% originating from the power-suppressed terms. This induces an effect of approximately 1% on the decay rate  $\Gamma(H \rightarrow gg)$ .

Fig. 7 shows the result for  $\delta\bar{\Gamma}^{\text{NNLO}}$  and  $\delta\Gamma^{\text{NNLO}}$ . Similarly to the NLO result one observes a reduction of the size of the mass corrections. This is particularly pronounced in the case of the  $\overline{\text{MS}}$  scheme where the curves involving terms up to order  $\bar{\tau}^1$  and  $\bar{\tau}^2$  lie on top of each other and coincide with the leading term up to  $\bar{\tau} \approx 0.4$  ( $M_H \approx 220$  GeV). These considerations provide a strong motivation to consider the total decay rate where the complete LO result is extracted. Furthermore, due to the similarity to the production of Higgs bosons in the gluon fusion channel it can be expected that there the mass corrections are also at the few percent level — below the current uncertainties from the parton distribution functions [12–14, 27].

Let us finally mention that the numerical effect of the power-suppressed terms computed in this paper are comparable to the leading  $M_t$ -term at NNNLO (cf. Eq. (11)).

At this point it is interesting to consider the dependence of  $\Gamma(H \rightarrow gg)$  on the renormalization scale  $\mu$ . In Fig. 8 the LO (dashed), NLO (dash-dotted), NNLO (solid) and NNNLO (dotted) result is shown for  $\mu$  between 10 GeV and 1 TeV where for the LO curve the exact result has been used. The NLO and NNLO curve include terms of order  $\tau^5$  and  $\tau^2$ , respectively. As input for our numerical studies we use  $\alpha_s(M_Z) = 0.118$ ,  $M_Z = 91.1876$  GeV [28],  $M_t = 170.9$  GeV [29] and  $M_H = 120$  GeV. The renormalization group equations are solved with the help of the program `RunDec` [30].

It is interesting to note that around  $\mu = 40$  GeV the NNLO curve shows a local maximum

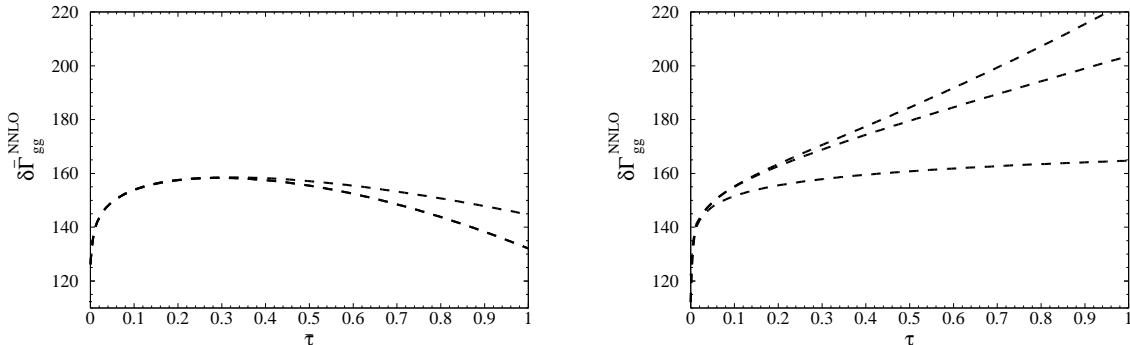


Figure 7:  $\delta\Gamma_{gg}^{\text{NNLO}}$  (left) and  $\delta\Gamma_{gg}^{\text{NNLO}}$  (right) as a function of  $\bar{\tau}$  and  $\tau$ , respectively, where successively higher orders are included. For the renormalization scale  $\mu^2 = M_H^2$  has been chosen.

where the decay rate is independent of  $\mu$ . For  $\mu = 50$  GeV the NNLO corrections vanish (crossing between dash-dotted and solid line) which hints for a good convergence of perturbation theory. This is further supported by the smallness of the NNNLO corrections (dotted) which show a very flat  $\mu$ -dependence over the whole range considered in Fig. 8.

## 4 Conclusions

In this paper the NNLO corrections to the gluonic decay width of the Higgs boson in the intermediate mass range is considered. With the help of an automated asymptotic expansion three terms in the large- $M_t$ -limit have been obtained. It is demonstrated that our result is equivalent to an exact calculation at least up to  $M_H = M_t$ . For  $M_H = 120$  GeV the NNLO term which changes by about 9% due to the new corrections induces a 1% correction to the total gluonic decay rate. The situation is different if the complete top quark mass dependence of the leading order result is factored out. In this case the power-suppressed corrections become smaller. This is in particular true for top quark masses in the  $\overline{\text{MS}}$  scheme where for Higgs boson masses up to 220 GeV the full result is given by the leading term in the large  $M_t$ -expansion. This observation has possible implications for the Higgs boson production via gluon fusion where only the leading order term in  $M_H/M_t$  is available. In case the expansion for  $M_H \ll M_t$  shows a similar behaviour the uncertainty induced by the unknown power-suppressed terms is negligible.

## Acknowledgements

We would like to thank Robert Harlander for useful comments and carefully reading the manuscript. This work was supported by the BMBF through 05HT6VKA and by the DFG through SFB/TR 9.

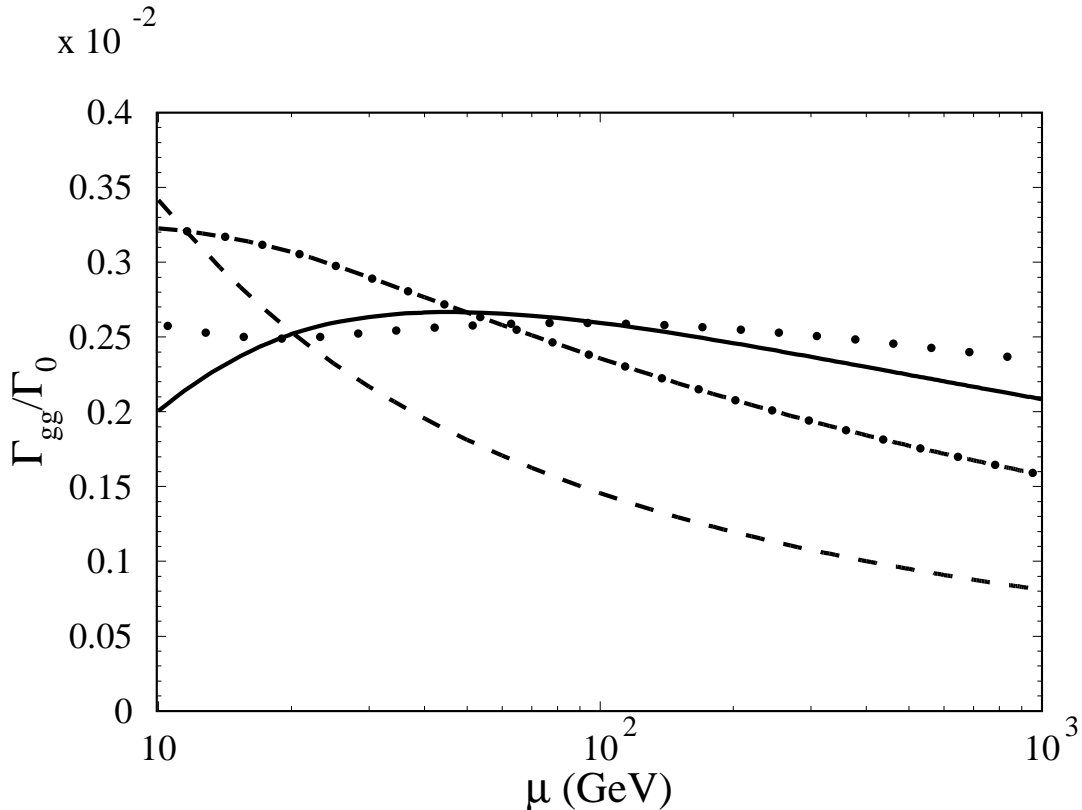


Figure 8:  $\Gamma_{gg}/\Gamma_0 \equiv \Gamma(H \rightarrow gg)/\Gamma_0$  as a function of  $\mu$  with  $\Gamma_0 = G_F M_H^3 / (36\pi\sqrt{2})$ . The LO, NLO and NNLO results are shown as dashed, dash-dotted and solid lines. The dotted curve also includes the leading top quark mass dependent term at NNNLO [11].

## References

- [1] J. R. Ellis, M. K. Gaillard and D. V. Nanopoulos, Nucl. Phys. B **106** (1976) 292.
- [2] M. A. Shifman, A. I. Vainshtein, M. B. Voloshin and V. I. Zakharov, Sov. J. Nucl. Phys. **30** (1979) 711 [Yad. Fiz. **30** (1979) 1368].
- [3] T. Inami, T. Kubota and Y. Okada, Z. Phys. C **18** (1983) 69.
- [4] S. Dawson and R. P. Kauffman, Phys. Rev. Lett. **68** (1992) 2273.
- [5] A. Djouadi, M. Spira and P. M. Zerwas, Phys. Lett. B **264** (1991) 440.
- [6] D. Graudenz, M. Spira and P. M. Zerwas, Phys. Rev. Lett. **70** (1993) 1372.
- [7] S. Dawson and R. Kauffman, Phys. Rev. D **49** (1994) 2298 [arXiv:hep-ph/9310281].

- [8] M. Spira, A. Djouadi, D. Graudenz and P. M. Zerwas, Nucl. Phys. B **453** (1995) 17 [arXiv:hep-ph/9504378].
- [9] K. G. Chetyrkin, B. A. Kniehl and M. Steinhauser, Phys. Rev. Lett. **79** (1997) 353 [arXiv:hep-ph/9705240].
- [10] M. Steinhauser, Phys. Rept. **364** (2002) 247 [arXiv:hep-ph/0201075].
- [11] P. A. Baikov and K. G. Chetyrkin, Phys. Rev. Lett. **97** (2006) 061803 [arXiv:hep-ph/0604194].
- [12] R. V. Harlander and W. B. Kilgore, Phys. Rev. Lett. **88** (2002) 201801 [arXiv:hep-ph/0201206].
- [13] C. Anastasiou and K. Melnikov, Nucl. Phys. B **646** (2002) 220 [arXiv:hep-ph/0207004].
- [14] V. Ravindran, J. Smith and W. L. van Neerven, Nucl. Phys. B **665** (2003) 325 [arXiv:hep-ph/0302135].
- [15] M. Steinhauser, arXiv:hep-ph/9612395.
- [16] V. A. Smirnov, *Applied Asymptotic Expansions in Momenta and Masses*, Springer-Verlag (2001).
- [17] R. Harlander, T. Seidensticker and M. Steinhauser, Phys. Lett. B **426** (1998) 125 [hep-ph/9712228].
- [18] T. Seidensticker, arXiv:hep-ph/9905298.
- [19] P. Nogueira, J. Comput. Phys. **105** (1993) 279.
- [20] J. A. M. Vermaseren, arXiv:math-ph/0010025.
- [21] M. Steinhauser, Comput. Phys. Commun. **134** (2001) 335 [arXiv:hep-ph/0009029].
- [22] S. A. Larin, F. V. Tkachov and J. A. M. Vermaseren, NIKHEF-H-91-18 (unpublished).
- [23] M. Tentyukov, H. M. Staudenmaier and J. A. M. Vermaseren, Nucl. Instrum. Meth. A **559** (2006) 224;  
see also <http://www-ttp.physik.uni-karlsruhe.de/~parform>.
- [24] M. Tentyukov and J. A. M. Vermaseren, arXiv:hep-ph/0702279.
- [25] S. A. Larin, T. van Ritbergen and J. A. M. Vermaseren, Phys. Lett. B **362** (1995) 134 [arXiv:hep-ph/9506465].
- [26] N. Gray, D. J. Broadhurst, W. Grafe and K. Schilcher, Z. Phys. C **48** (1990) 673.

- [27] S. Moch and A. Vogt, Phys. Lett. B **631** (2005) 48 [arXiv:hep-ph/0508265].
- [28] Particle Data Group The Review of Particle Physics: <http://pdg.lbl.gov/>.
- [29] [CDF Collaboration], arXiv:hep-ex/0703034.
- [30] K. G. Chetyrkin, J. H. Kühn and M. Steinhauser, Comput. Phys. Commun. **133** (2000) 43 [arXiv:hep-ph/0004189].